Anees AHMAD[1], Davide FUGAZZA[1]

Fusion of Sentinel-1 interferometric coherence and Sentinel-2 MSI for debris-covered glacier boundary delineation: Case study of Batura, Passu, Ghulkin, and Gulmit Glaciers, Pakistan

Abstract: Ahmad A., Fugazza D., *Fusion of Sentinel-1 interferometric coherence and Sentinel-2 MSI for debris-covered glacier boundary delineation: Case study of Batura, Passu, Ghulkin, and Gulmit Glaciers, Pakistan.* (IT ISSN 0391-9838, 2023). Glaciers are vital freshwater reservoirs on Earth, and Pakistan is home to some of the world's largest mid-latitude glaciers, which greatly contribute to the country's economy. The accelerated melting of glaciers worldwide due to climate change underscores the significance of regular monitoring. However, many glaciers especially in the Hinduskuh and Karakoram are covered with debris, making it challenging to rely solely on optical satellite imagery for monitoring changes and creating glacier inventories for change detection. Consequently, studies in these regions often yield conflicting results. This study presents a new and robust approach that combines interferometrically derived synthetic aperture radar (InSAR) coherence with optical multispectral data in an object-based image analysis (OBIA) framework to delineate debris-covered glacier outlines accurately. InSAR coherence is capable of detecting temporally decorrelated surfaces, such as glaciers, regardless of their surface type (ice or debris). It effectively separates these surfaces from the highly coherent surrounding areas. OBIA offers numerous benefits compared to conventional classification methods because it can leverage multiple data sources and process data contextually and hierarchically. To the best of our knowledge, this approach has not been used previously for glacier delineation. This integrated method resulted in an overall glacier accuracy of 94.87% compared to manually corrected outlines. This highlights the excellent performance of this integrated approach, which showed minimal misclassifications and robustness against conventional methods. Furthermore, a comparative analysis involving Sentinel-2 multispectral data and previous glacier inventories highlighted the potential of the proposed robust processing chain, emphasizing its capability to consistently update the boundaries of land-terminating glaciers on a large scale.

Key words: InSAR Coherence, Sentinel-2, Object-based image analysis, Glaciers delineation, Karakoram.

INTRODUCTION

Mountain glaciers are essential sources of freshwater for major rivers worldwide, providing crucial support for irrigation and contributing to food production and human needs. Northern Pakistan is recognized as the home to some of the largest mid-latitude glaciers, which are pivotal for the country's economy, particularly in facilitating hydropower generation and agriculture with their meltwater (Anwar and Iqbal, 2018; Moazzam *et al.*, 2022; Shafique *et al.*, 2018). Glaciers are highly responsive to fluctuations in temperature and precipitation: a study by Cogley (2017) has highlighted the rapid shrinkage of glaciers in the high mountains of Asia. The accelerated melting of glaciers, driven by global warming, has caused

an extensive retreat (Kraaijenbrink *et al.*, 2017). Another cause of accelerated melting is the accumulation of debris in glaciated areas (Kraaijenbrink *et al.*, 2016), resulting in a landscape that closely resembles its surroundings causing a great challenge for the efficiency of optical remote-sensing technologies to distinguish and analyze the modified glacier-covered areas accurately (Smith *et al.*, 2015). Thus, a comprehensive understanding of glacier attributes, particularly their extent, is a fundamental requirement for a range of scientific investigations. However, glacier inventories like GAMDAM (Glacier Area Mapping for Discharge from the Asian Mountains) and ICIMOD (International Centre for Integrated Mountain Development) show inconsistencies, particularly in the measurement of debris-covered glaciers. This discrepancy was observed in the case study of Batura, Ghulkin, and Gulmit Glaciers as shown in fig. 1, and highlights the need for further investigation to address these inconsistencies, ensuring a more accurate interpretation of

[1] *Department of Environmental Science and Policy, University of Milan, 20133 Milan, Italy.*

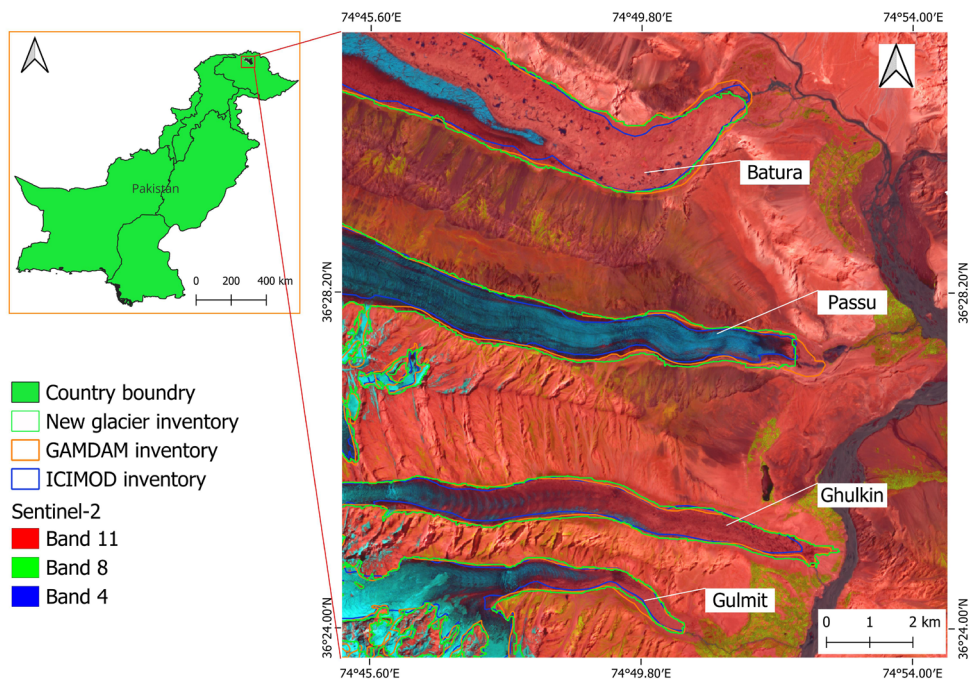*Corresponding author: Anees Ahmad (anees.ahmad@unimi.it)*

Figure 1 - The locations of Batura, Passu, Ghulkin, and Gulmit glaciers within the Hunza Basin in north Pakistan. The inset on the right offers a detailed view of the lower catchment area, including glacier boundaries as outlined in previous inventories.

glacier behavior in regions characterized by debris-covered glaciers. Such discrepancies arise due to variations in generation methods, operators, and data used in the abovementioned inventories. Different techniques have been devised for glacier outline mapping through optical (Byers *et al.*, 2019; Jabbar *et al.*, 2020; Mazhar *et al.*, 2018; Ranzi *et al.*, 2004), thermal (Aubry-Wake *et al.*, 2023; Shukla *et al.*, 2010) and high-resolution orthophotography (Salvatore *et al.*, 2015) remote-sensing data. However, the usefulness of thermal data is constrained by the limited spatial resolution of available satellite products and when delineating thick supraglacial debris-covered terminus (Alifu *et al.*, 2015), whereas optical sensors face limitations in acquiring cloud-free and well-illuminated images (Lippl *et al.*, 2018).

InSAR (Interferometric SAR) coherence, as a complementary approach has gained attention in glacier mapping (Arigony-Neto *et al.*, 2007; Lippl *et al.*, 2018; Mohajerani *et al.*, 2021). InSAR coherence shows the complex relationship between two synthetic aperture radar (SAR) images, indicating the consistency of the backscatter signal over time. Its range of values spans from 0 to 1, where 0 represents full decorrelation and 1 indicates stability. The temporal changes resulting from a glacier's movement due to gravity can lead to reduced coherence. This reduction is a key indicator for delineating debris-covered glaciers, independent of their spectral characteristics. However, the complex topography in mountainous regions, such as the Himalayas, Karakoram, and Hindukush, poses challenges with layover and foreshortening, causing a lack of

signal return to the sensor over large areas (Frey *et al.*, 2012). Some studies like Atwood *et al.* (2010), integrated coherence with slope, size, and morphological filters to outline glacier extent. However, instances of data voids due to rugged terrain led to manual adjustments, as observed in the work by Frey *et al.* (2012). Challenges arising from distinguishing glacier areas from similarly coherent non-glaciated regions, as encountered by Wu *et al.* (2012), were addressed through advanced texture analysis. Although these methods have been instrumental in mapping glacier boundaries, they are mostly limited to the tongue of the glacier. Accurate delineation of the entire glacier, without manual correction, remains challenging in many regions. This study aims to develop an integrated approach for robust and accurate glacier delineation. We stacked an InSAR coherence image with an optical image to classify glaciers based on coherence and near-homogeneous objects using the OBIA (Object-Based Image Analysis) method. OBIA offers a promising methodology, focusing on near-homogeneous objects for classification rather than pixels. This approach offers flexibility in setting classification rules, taking into account spatial characteristics and contextual information. Additionally, OBIA allows the integration of multi-source data, such as optical satellite imagery, InSAR data, and DEMs (digital elevation model). Using OBIA in glacier classification, leveraging optical, topographic, and InSAR coherence data, provides a robust methodology for remote sensing applications.

BACKGROUND

OBIA is a comprehensive approach for spatial information extraction, merging image processing with GIS (Geographical information system) functionalities. Unlike conventional pixel-based techniques, which focus solely on spectral characteristics, OBIA segments pixels into homogeneous objects, enhancing the analysis of complex natural features like glaciers. Working on the object level allows the incorporation of various properties, including spectral, spatial, textural, hierarchical, and contextual, derived from multiple data sources. This methodological framework assists the computer-based interpretation of intricate classes, presenting a promising opportunity in remote sensing and geographic information sciences. In our study, OBIA is used on an InSAR coherence image fused with an optical image to classify debris-covered ice, displaying its superiority over pixel-based classification techniques, particularly in delineating glaciers under debris-covered conditions. Combining the coherence band with optical bands helps distinguish between coherent surfaces and non-coherent features, such as debris-covered glaciers. Also, it helps to overcome foreshortening and layover effects by altering band combinations. Previous studies such as Rastner *et al.* (2014) and Kraaijenbrink *et al.* (2016) demonstrated the effectiveness of OBIA in classifying glaciers. This integrated approach of InSAR and optical data using an object-based approach proves advantageous, especially when dealing with high-resolution imagery or combining data from various sources.

STUDY AREA

The study area is located in the upper Hunza Valley, Huza Nagar district, Gilgit-Baltistan, within the central Karakoram in northern Pakistan as shown in fig. 1. Elevation within the study region ranges from 3000 to 7900 meters a.s.l., as determined by data from the Shuttle Radar Topography Mission (SRTM) digital elevation model (DEM). The region features prominent peaks such as Distaghil Sar (7885 m a.s.l), Batura Muztagh (7795 m a.s.l), and Passu Sar (7476 m a.s.l). Extensive glaciers, such as the Hispar Glacier and the Batura Glacier surround these high peaks in the area. These glaciers primarily feed the Hunza Nagar River, the area's main water source. Hunza Nagar district experiences the influence of the westerlies and the Indian Monsoon during the summer season and has a temperate climate, with average low and high temperatures of 16°C and 35.9 °C respectively in Ali Abad in the valley floor. The annual average rainfall is 136.2 mm, ranging from a minimum of 2.1 mm in November to a maximum of 28.3 mm in April (Shafique *et al.*, 2018).

The selected glaciers for this study are Batura, Passu, Ghulkin, and Gulmit. Batura Glacier is around 59 kilometers long and is one of the longest outside the polar regions. To its south lie the Passu, Ghulkin, and Gulmit Glaciers. Among these glaciers, Passu Glacier is clean without debris cover, while the Batura, Ghulkin, and Gulmit Glaciers are covered with debris, as shown in fig. 1. The University of Mian and EVK2 CNR have created a new glacier inventory of Pakistan (referred to as "new glacier inventory" in this study) using Sentinel 2 imagery acquired in 2022 (Diolaiuti *et al.*, 2024). Based on this inventory, the Batura Glacier covers a total area estimated to be 273.3 km², with elevations ranging from 2622 m to 7775 m a.s.l. and a slope of 21.6°. The Passu Glacier spans approximately 52.4 km², with elevations ranging from 2688 m to 7645 m a.s.l. Furthermore, the Ghulkin Glacier ranges from 2456 m to 7087 m a.s.l. in elevation, covering an area of 23.2 km², while the Gulmit Glacier covers an area of 11.1 km².

MATERIALS AND METHODS

Data

Sentinel 1 single look complex (SLC) imagery and cloud-free (< 5%) optical imagery from Sentinel 2 multi-spectral instrument (MSI) imagery acquired in July 2022 were used. The European Space Agency provides both optical Sentinel-2 MSI and InSAR Sentinel-1 sensor SLC data for earth observation free of cost, rendering them well-suited for environmental analyses. The Sentinel-2 sensor offers 13 distinct spectral bands, ranging from the visible spectrum to shortwave infrared, with wavelengths between 443 nm and 2190 nm. In terms of spatial resolution, Sentinel-2 captures three distinct resolutions: 10 meters for the visible and near-infrared bands, 20 meters for the red-edge and shortwave infrared bands, and 60 meters for the atmospheric correction bands. This blend of high spectral and spatial resolution improves the sensor's capability and facilitates the use of advanced algorithms for accurate spectral identification of glaciers, as highlighted by (Kääb *et al.*, 2016; Paul *et al.*, 2016). In contrast, Sentinel-1 is an active radar sensor and captures imagery within the C-band. Interferometric Wide (IW) swath mode of sentinel 1 is the primary mode used over land, covering a 250 km swath at a spatial resolution of 5 m × 20 m. It employs the Terrain Observation with Progressive Scans SAR (TOPSAR) acquisition principle to capture three sub-swaths. This technique electronically steers the beam both in the range, similar to ScanSAR, and azimuthally from backward to forward for each burst. This dual steering minimizes scalloping, resulting in uniform image quality throughout the swath. The TOPSAR mode supersedes the conventional ScanSAR, maintaining equivalent coverage

Table 1- Sentinel-1 and -2 data utilized in this study for glacier classification.

Acquisition Date	Image ID	Satellite	Spatial resolution (m)
04-07-2022	S2B_MSIL1C_20220704T054649_N0400_R048_T43SDA_20220704T081851.SAFE	Sentinel-2	10
09-07-2022	S1A_IW_SLC__1SDV_20220709T125748_20220709T125816_044024_054146_7026.SAFE	Sentinel-1	5 × 20
21-07-2022	S1A_IW_SLC__1SDV_20220721T125748_20220721T125816_044199_054682_B890.SAFE	Sentinel-1	5 × 20

and resolution while achieving consistent image quality, as measured by the signal-to-noise ratio and distributed target ambiguity ratio (Meyer, 2020). The Interferometric Wide Swath (IW) mode of the C-band of Sentinel-1 was chosen for estimating SAR coherence. The temporal baselines between SAR pairs hold significance, impacting the overall image coherence and potentially influencing co-registration quality. It is vital to acknowledge that seemingly minor factors such as solid precipitation or wind drift and vegetation growth during acquisition intervals can exert substantial influence on co-registration accuracy, leading to compromised coherence even in cases without actual surface movement (Villarroya-Carpio *et al.*, 2022). The optical imagery and radar data were obtained from the Copernicus website, specifically focusing on acquiring data with minimal cloud cover and fresh snow cover. Therefore, imagery from July to September was examined for this purpose. The temporal baseline of the SAR imagery of descending order was 12 days. The dataset utilized in this research is detailed in table 1.

Methods

In this study, we propose a novel approach to stack InSAR coherence with optical multispectral data. To the best of our knowledge, this approach is not been used previously on Sentinel-2 optical and Sentinel-1 InSAR combined data for the delineation of debris-covered glaciers. The methodology can be divided into three main sections i.e., i) estimation of coherence from SAR SLC images, ii) combining Sentinel 1 InSAR image with Sentinel 2 optical bands, and iii) Segmentation of the InSAR coherence and Sentinel 2 optical composite image based on similar pixels. Fig. 2 illustrates the flowchart outlining the methodology utilized for estimating coherence and extracting the glacier outlines.

Coherence estimation

The process involved employing the processing tools in SNAP (Sentinel Application Platform) software for automated calculations. Interferometric processing involves combining pairs of SLC images at VV polarization into interferograms as the VV channel is more suitable for variation and returns higher coherence compared to HH polarization (Villarroya-Carpio *et al.*, 2022). Before generating the interferogram, a crucial step involves co-registering the Sentinel-1 SLC split pairs (reference and secondary) within the sub-swath (fig. 2 p1). This process utilizes the orbits of the two products and a Shuttle Radar Topography Mission (SRTM) 1 Arc-Second DEM for geometric correction, ensuring accurate interferogram calculations. Refining the interferogram involves subtracting the topographic phase, achieved by "radar coding" the DEM to the interferogram area and subtracting it from the complex interferogram. To address the inherent speckle noise in SLC images, a combination of Goldstein Phase Filtering and the multilooking method was applied. A scene is captured multiple times in a SAR image, from slightly different angles. Each of these captures is called a "look." Multi-looking involves combining several of these looks into a single processed image. The multilooking method not only reduces noise but also generates square ground pixels for a more accurate representation (Holobâcă *et al.*, 2021). This process decreases spatial resolution by blending finer details. Consequently, while the image becomes clearer, the ability to discern small features is reduced (Braun and Veci, 2021). This technique entails averaging multiple looks or samples within a SAR image pixel, usually along both range and azimuth directions. By doing so, it creates a smoother and more comprehensible image, thereby improving image quality and facilitating the identification of features and patterns within the SAR data.

The last step in SNAP processing involves range Doppler terrain correction. To create a layover and shadow mask the SAR simulation terrain correction operator was used. This step is essential because the layover effect causes the signal reflected from the top of the mountain to reach the receiver before the signal from the bottom, leading to inversion on the fore-slope. Removing the shadow effect simultaneously conceals information from the backslope, improving the accuracy of the processed SAR data. At the terrain correction stage, the coherence images were resampled to a pixel size of 10 meters to enable seamless stacking with optical multispectral data for the delineation of glacier boundaries.

Various factors contribute to the loss of coherence between SAR images, including steep slopes reducing signal-to-noise ratio and vegetated surfaces introducing decorrelation through volume scattering (Massom and Lubin, 2006; Villarroya-Carpio *et al.*, 2022). Large baselines result in reduced coherence, and extended time lags
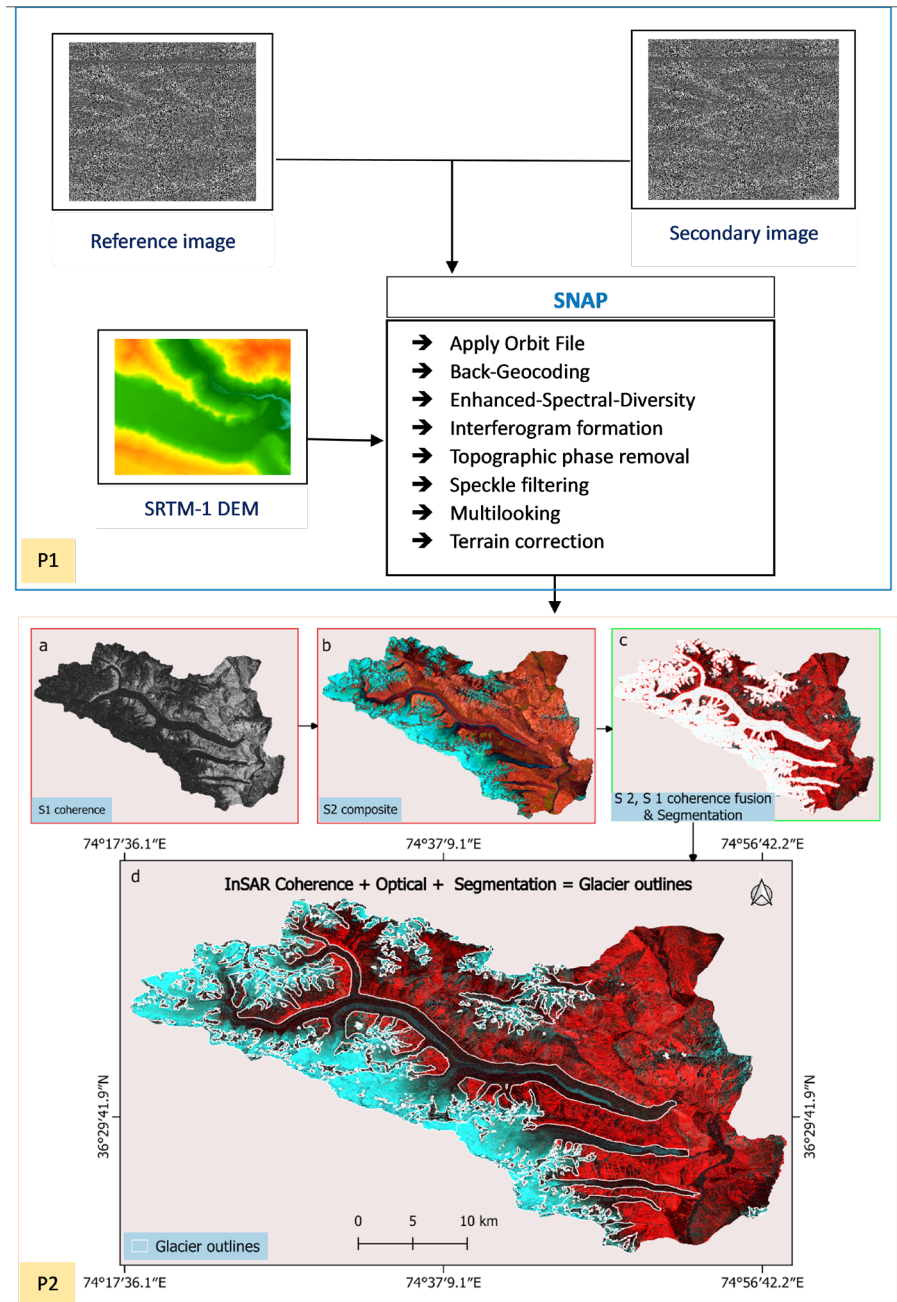
Figure 2 - The methodology for creating glacier outlines using InSAR coherence estimation and optical composite. Initial processing steps (p1) were conducted in SNAP, followed by further processing in QGIS (p2). Within QGIS, images 'a' and 'b' were stacked to produce 'c' upon which OBIA was performed to derive glacier outlines 'd'.

between images lead to the same effect (Holobâcă *et al.*, 2021). In glacial environments, notable transformations like glacier surges, substantial melting, or snow accumulation lead to coherence reduction. Addressing these issues involves careful selection of the season and SAR images, supplemented by consultation with meteorological data. Optimal coherence values are often observed during peak ablation season which is from mid-July to mid-August (Lu and Freymueller, 1998). The 12-day repeat orbit pattern of Sentinel-1 serves a crucial function in regulating the minimum time interval necessary when employing ascending or descending pairs, since the loss

of Sentinel-1B. It ensures the effective monitoring of glacier movement while mitigating coherence loss for other land-use categories.

The time required for data acquisition, processing, and analysis largely depends on the system's specifications and internet speed. On an average i7 system with 20 GB of RAM and a 2.7 GHz processing capacity, and with typical internet speed, it can take up to 24 hours to process a single Sentinel-1 scene. We successfully processed imagery covering approximately 80,971 km² (encompassing nearly the entire KHK region of northern Pakistan) using Sentinel-1 data and estimated the coherence for the area.

Image fusion

Both InSAR and optical data have their advantages and disadvantages. One limitation of InSAR is its performance in challenging terrain. On the other hand, optical data often show discrepancies of 30% or more in the spectral classification of debris-covered ice compared to manually corrected outlines (Robson *et al.*, 2015). This discrepancy arises mainly due to the similar spectral signatures of glacier debris and the surrounding bedrock. To address these issues, we utilized a combination of InSAR and optical bands. A single coherence image using SNAP was generated. Subsequently, the build raster tool within QGIS was utilized to merge the visible bands (bands 2, 3, and 4), NIR band (band 8), and SWIR band (band 11) of the Sentinel-2 scene with the coherence image, all at a spatial resolution of 10 meters.

By fusing the coherence band with the optical bands, we aimed to distinguish between coherent surfaces and non-coherent features, such as debris-covered glaciers, within the image by altering band combinations. Additionally, optical bands such as band 11 and band 8 aided in the differentiation of clean ice from surrounding features. The integration of InSAR with optical bands not only facilitated the removal of layover and foreshortening effects in the images but also addressed one of the principal challenges encountered when using InSAR in such topographic areas. Moreover, this combined approach assisted in distinguishing low-coherence features, such as vegetation cover and water, within the image.

Segmentation

OBIA represents a spatially precise methodology for extracting information and merging image processing with GIS capabilities (Blaschke, 2010). Segmenting images into near-homogeneous objects is a crucial stage in OBIA. This process involves grouping pixels into objects in a bottom-up manner, and various hierarchical levels can be formed by merging individual objects. The spectral analysis focused on delineating glacier ice/snow, glacier debris, and rocky slopes. To differentiate glacier debris from the surrounding rocks, a new dataset was generated resulting in a novel multiband image stack. The coherence image was stacked with the optical image to create a multi-band image, clearly highlighting debris-covered glaciers. The optimal approach for differentiating the clean glacier involves utilizing spectral reflectance from the optical image, while the debris-covered part can be identified by coherence estimation. Subsequently, a segmentation classification algorithm was implemented on this updated multi-band dataset to group pixels based on their proximity and similarity in response to spectral reflectance and coherence, thus enhancing the differentiation process (see fig. 3).

Rastner *et al.* (2014) highlighted that the effectiveness of OBIA is greatly influenced by the initial choice of parameters made during the segmentation process. The OBIA segmentation process was performed in QGIS,
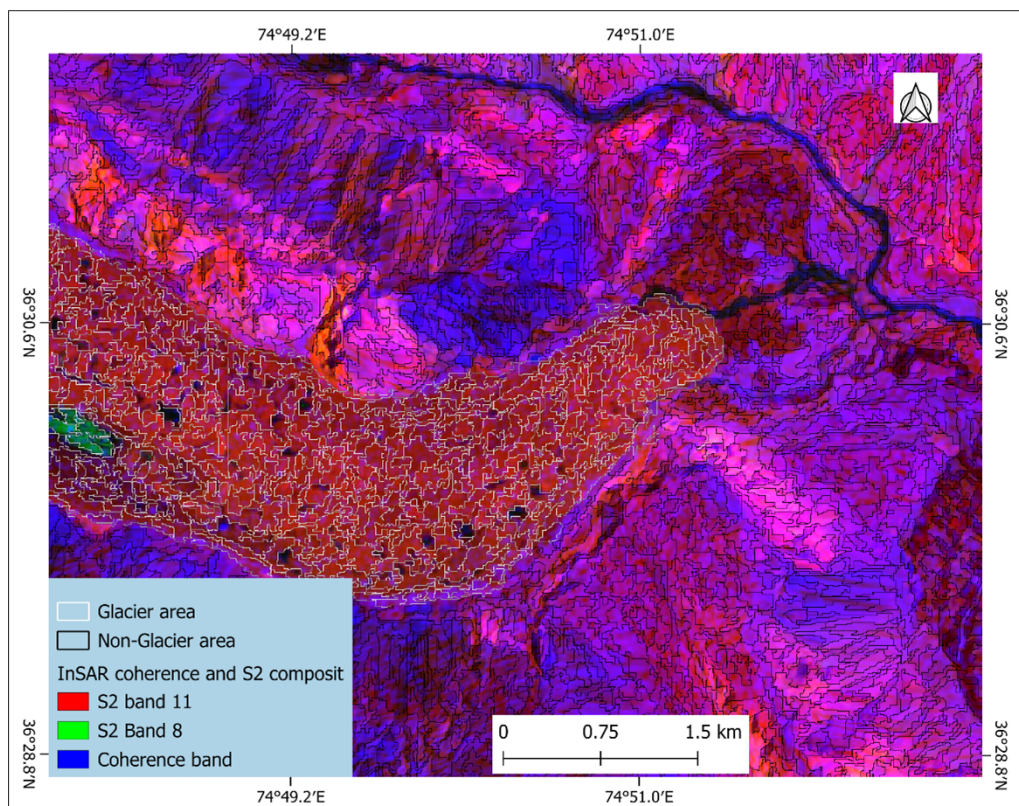

Figure 3 - Illustration of the segmentation using combined InSAR and optical imagery. The InSAR coherence image is displayed in the blue band, Sentinel-2 Band 8 in the green band, and Sentinel-2 Band 11 in the red band. After classification, glacier segments are shown in white, while non-glacier areas are represented in black.

utilizing the Orfeo Toolbox (OTB) plugin, which incorporates the multi-resolution segmentation algorithm, that integrates spectral, geometric, and texture properties with predefined and customizable parameters governing size, shape, and similarity to neighboring segments. Essential parameters include the segmentation algorithm, dictating the method for partitioning the image into segments, spatial radius, determining the spatial scale of segmentation, and range radius, which influences spectral variation within segments. Additionally, the optional minimum segment size parameter allows users to filter out small segments, aiding in noise reduction and artifact removal from the segmentation results.

In this study, we applied the mean-shift (multi-threaded) segmentation algorithm. We kept a spatial radius, representing the neighborhood radius, at a value of 5. Similarly, the range radius, signifying the radius in the multispectral space and expressed in radiometry units, was retained at 10, with a mode coverage of 0.1000. Additionally, the minimum size of a region during segmentation was set to 50 pixels, facilitating the merging of smaller clusters with the nearest neighboring cluster based on radiometric similarity. As a result of this step, a polygonal vector format (shapefile) was created and glacier polygons were assigned with a value; this way the glacier boundary was delineated from adjacent non-glacier areas. The parameters were selected with reference to Michel *et al.* (2015) and were adjusted according to the spatial resolution to match the specific characteristics of the study area, optimizing the balance between detail and noise reduction for precise glacier mapping. While these settings are customized for our particular environment, they can be modified for use in other locations.

RESULTS

The glacier outlines generated using OBIA were compared against the new glacier inventory created by the University of Milan using Sentinel 2 data. Our observation indicates that the debris cover on the Batura, Ghulkin, and Gulmit glaciers exhibits reduced coherence. This suggests that interferometric coherence is a valuable metric for distinguishing between active debris-covered glaciers and areas of bedrock. While acknowledging the possibility of variations in other regions and recognizing the impact of errors associated with layover and shadow areas on overall performance, it is recommended to consider integrating data from multiple image directions in such cases. The results derived from Sentinel 2 imagery (new glacier inventory) are better than those from Landsat used in the GAMDAM inventory (see fig. 4), primarily due to the ability to identify glaciers more effectively due to the availability of multiple spectral bands and higher spatial resolution (Anwar and Iqbal, 2018). Delineating glacier boundaries becomes challenging when using coarse-resolution imagery.
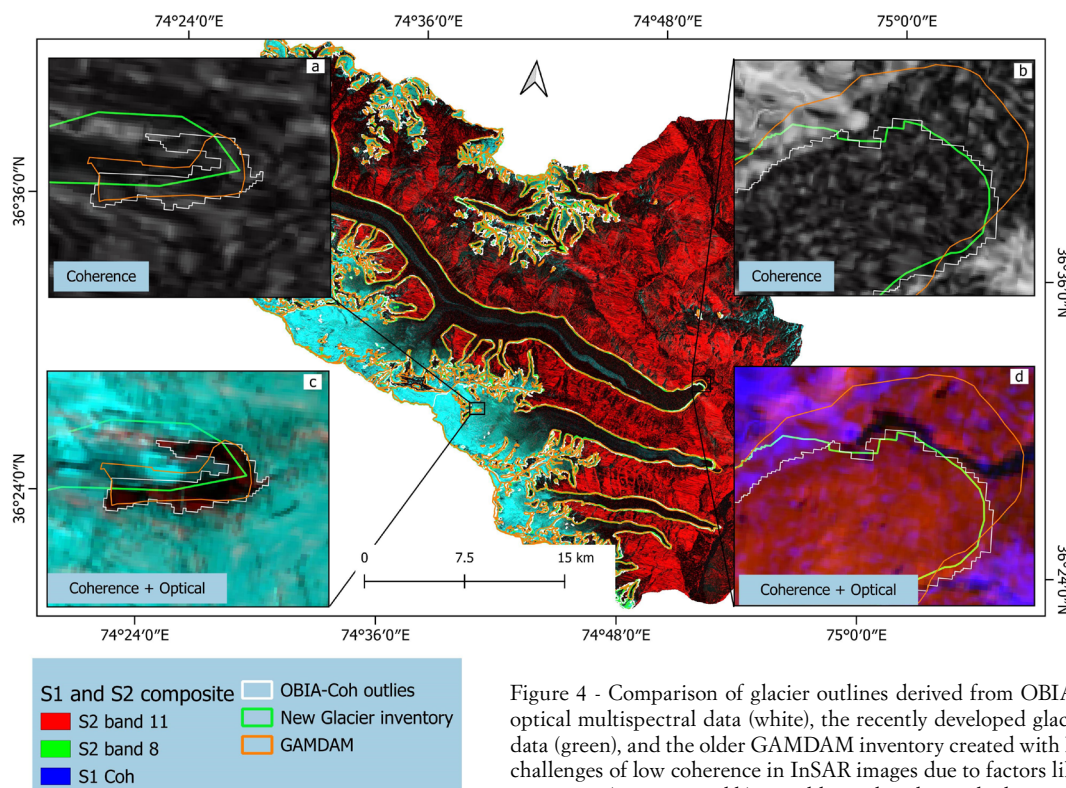

Figure 4 - Comparison of glacier outlines derived from OBIA using combined InSAR and optical multispectral data (white), the recently developed glacier inventory using Sentinel-2 data (green), and the older GAMDAM inventory created with Landsat imagery (yellow). The challenges of low coherence in InSAR images due to factors like shadow, layover, water, and vegetation (seen in a and b) are addressed in the stacked images (c and d).

In the coherence image, the region with low coherence covers both the debris-covered and clean ice of the glacier, while the high coherence area represents non-glacier regions. However, at the terminus of the Batura glacier, there were instances of low coherence blocks likely caused by flowing water and vegetation growth (fig. 4b). Fig. 4 shows that layover and foreshortening effects caused by rough terrain (fig. 4a) and low coherence caused by vegetation and water bodies (fig. 4b) can be removed in an InSAR and optical multispectral data. This helped during the segmentation process to accurately delineate glacier boundaries.

To evaluate the accuracy of our glacier outlines we conducted an assessment based on the recently developed inventory by the researchers at the University of Milan using imagery acquired in 2022. Unlike the previous glacier inventories, our approach incorporated InSAR coherence data to determine the extent of glacier ice beneath the debris cover while creating glacier outlines. The OBIA outlines derived from InSAR coherence and optical data were compared with the reference glacier inventory (new inventory), using percentages of deviation to assess accuracy.

To assess the accuracy of the delineated glacier outlines, a buffer zone of 200 meters was established around the debris-covered sections of Batura Glacier of Ghulkin and Gulmit Glaciers, taking into account both the glacier dimensions and the valley width. Four cases were considered: (a) 'true positive', which denotes the overlap of the glacier area delineated from the automatic process with the glacier area from the manually corrected data, (b) 'false positive', which corresponds to the glacier area mapped exclusively by our processing, (c) 'true negative', which pertains to pixels classified as no-glacier in both instances (correctly unassigned), and (d) 'false negative', which represents the region classified as a glacier solely by the reference dataset. Compared to the reference datasets, the OBIA approach, which utilizes optical and coherence data, was able to detect debris-covered areas, water, and vegetation (see fig. 5). However, this led to some false positive detections when compared to the reference data. These areas were meticulously checked and some of the area was included in the glacier outlines, resulting in a larger estimated glacier area compared to the previous inventory (table 2). As illustrated in fig. 6, 96.8% of the area of Batura Glacier was correctly classified compared to the reference inventory, while 94.6% of Passu Glacier and 94.7% and 93.4% of Ghulkin and Gulmit, respectively, were accurately classified.

Various studies, such as Anwar and Iqbal (2018) and Moazzam et al. (2022), have indicated anomalous and stable behavior among Karakoram glaciers, and the same pattern was also observed in our study. More precisely, Batura Glacier and Passu Glacier show signs of retreat when compared with previous inventory such as GAMDAM (fig. 4). Ghulkin appears to have undergone surging, and the Gulmit glacier is stable when compared to the GAMDAM inventory. The GAMDAM glacier inventory was completed in 2010 using Landsat ETM+ scene from 1999-2003 (Nuimura et al., 2015). Since then, it has been updated multiple times. The inventory was revised and expanded in 2015 using imagery from 1990-2010, reflecting improvements in data and methodology (Xie et al., 2023). The comparison of the studied glaciers against the previous inventory is given in table 3.
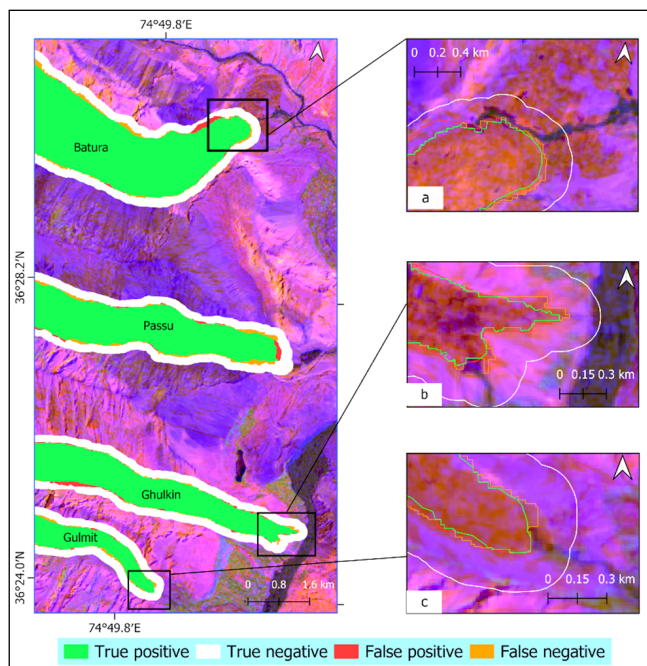

Figure 5 - The white polygons around each glacier represent the buffer zone for error analysis. Panels (a) to (c) display the insight maps of the Batura, Ghulkin, and Gulmit glaciers, respectively, demonstrating the accuracy of the adopted approach in this study.
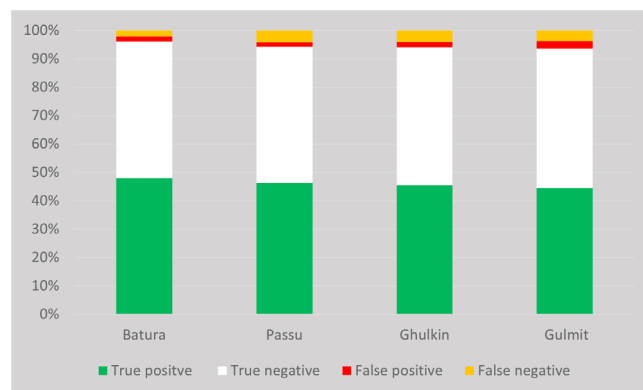

Figure 6 - The figure depicts the area and proportion categorized into four different classes (true positive, true negative, false positive, and false negative) compared to the reference inventory.

Table 2. Comparison of the areal extent of studied glaciers recorded in the reference glacier inventory (a) and our inventory (b). Areas are reported in km².

	Inventories	Batura	Passu	Ghulkin	Gulmit
a	New inventory	273.3	52.4	23.3	11.1
b	OBIA-Coherence glacier outlines	274.9	53	23.7	11.6

Table 3. Comparison of the studied glaciers between different glacier inventories. Areas are reported in km².

	ICIMOD inventory	GAMDAM inventory	New glacier inventory	OBIA-Coherence derived outlines
Batura glacier	236.4	275.5	273.3	274.9
Passu glacier	50.5	52	52.4	53
Ghulkin glacier	21.2	20.7	23.2	23.7
Gulmit glacier	9.1	11.5	11.1	11.6

DISCUSSION

In comparison to conventional methods, utilizing SAR data for delineating debris-covered glaciers offers several advantages: SAR data can be used effectively regardless of the time (day or night), and it operates independently of cloud cover, which often obstructs optical imagery. While optical imagery and DEMs are commonly employed for glacier outline delineation, especially in remote sensing applications, they may not accurately represent the boundaries of debris-covered glaciers, where debris-covered areas are challenging to delineate. Thermal bands can be used in mapping debris-covered glaciers due to their ability to capture variations in surface temperature. These variations help distinguish between ice, debris, and other materials on the glacier's surface. However, it also presents inaccuracies, e.g., owing to thermal contrasts in the shadow caused by the varying surface aspect and the lower spatial resolution it provides. In contrast, coherence maps derived from SAR data offer clear delineation of the boundaries of debris-covered glaciers, a task that proves difficult with optical imagery. The errors and uncertainties primarily stem from the accuracy of coherence estimation, which may vary when employing different estimation methods. Jiang *et al.* (2011) and Lippl *et al.* (2018) have highlighted the uncertainties with coherence estimation when using various estimation techniques. Moreover, vegetation and water bodies exhibit relatively similar coherence as glaciers. As a result, they contribute to misclassification in the coherence mask image, which may arise from vegetation cover near the glacier terminus. Combining optical data with InSAR coherence can significantly address this issue, and this challenge might be further mitigated by conducting observations at a shorter temporal baseline. However, fast-flowing glaciers, which can be distinguished from rivers and lakes, may still present some difficulties.

Utilizing Sentinel-1 InSAR coherence stacked with Sentinel-2 optical data for delineating debris-covered glaciers yields highly accurate results. This process requires examining various technical parameters to assess their impact on the accuracy of the results. Parameters such as the selection of temporal baselines to accommodate seasonal variations, assessment of spatial resolution effects, and evaluation of pre-processing techniques like radiometric and geometric corrections, speckle filtering, and terrain correction on coherence values are essential. In addition, determining optimal coherence thresholds for classification, exploring integration benefits of SAR and optical data, and validating results with ground truth data are crucial steps. Consideration of terrain characteristics, temporal dynamics, and sensitivity assessment, including error propagation from coherence estimation to final delineation, further enhances the sensitivity analysis, ensuring robust glacier mapping methodologies.

The literature on OBIA is rapidly expanding, leading to the emergence of sub-topics such as specific OBIA hierarchy and scale concepts (Addink *et al.*, 2007), segmentation for OBIA (Trias-Sanz *et al.*, 2008) and OBIA change detection (Gamanya *et al.*, 2009; Stow *et al.*, 2008). Its ability to integrate contextual information allows the removal and reclassification of clouds and shadows intersecting with glacier ice, reducing the need for extensive manual corrections. Moreover, OBIA efficiently separates objects into their constituent components, enabling the assignment of classes within a hierarchical structure. The hierarchical approach allows the representation of glaciers in distinct categories such as "clean ice" and "debris-covered ice", or "glacial lakes" including "pro-glacial lakes", "supra-glacial lakes", and "marginal-glacier lakes" (Nigrelli *et al.*, 2013; Robson *et al.*, 2015). OBIA's ability to handle optical, SAR, and DEM data simultaneously allows for the integration of multiple datasets to enhance the classification of debris-covered ice compared to conventional methods. It is important to note, that some methods such as the pixel-based classification methods are simpler and faster to execute compared to OBIA. However, OBIA on optical and InSAR coherence imagery is highly replicable and scalable, making it a valuable tool for large-scale classification, such as

glacier mapping. Its adaptability allows it to be customized to different regions by adjusting segmentation parameters to suit specific landscape characteristics and data quality. This ensures the method can be applied effectively across diverse geographic areas, including debris-covered glaciers in mountainous regions and other complex terrains. Moreover, the combination of optical and InSAR coherence data increases the analysis's accuracy, enabling precise delineation of features like glacier boundaries, regardless of surface conditions. The scalable nature of OBIA, along with the broad availability of Sentinel-1 and Sentinel-2 data, makes it an effective approach for consistent, large-scale studies. This method not only supports the creation of updated and reliable inventories but also enhances ongoing monitoring efforts, making it highly replicable and suitable for various environmental and geographic settings. Several studies have highlighted the effectiveness of Object-Based Image Analysis (OBIA) in distinguishing debris-covered ice from surrounding terrain, especially when combined with InSAR coherence and optical data. For example (Robson *et al.*, 2015) used OBIA on Landsat and ALO-SPALSAR combined multi-resolution images and reported a 30% improvement in accuracy over manual delineation. Thomas *et al.* (2023), in their study, achieved an overall 3% accuracy and 12% increase in accuracy over debris-covered glaciers compared to pixel-based image analysis using deep learning, highlighting OBIA's ability to manage complex spectral signatures and varying debris cover. These studies highlight the improved accuracy and reliability of OBIA in detecting and analyzing debris-covered glaciers using optical data. However, by integrating InSAR coherence with optical data, the accuracy and reliability of glacier mapping are further enhanced. As previously mentioned, InSAR coherence identifies stable and unstable surfaces, which, when combined with the spectral information from optical data, allows for more precise differentiation between debris-covered ice and non-glacier areas. Consequently, we achieved an overall accuracy of 94.87% when compared to a recently developed glacier inventory for the region.

CONCLUSION

In this study, we synergistically employed InSAR coherence and OBIA method on the InSAR and optical fused data to effectively and robustly outline both clean ice and debris-covered glaciers. Coherence data played a pivotal role in detecting surface movement on debris-covered glaciers, significantly improving outline detection, especially in challenging areas like glacier termini and slope contacts. This method also assisted in information retrieval from layover, foreshortening, and shadow areas while effectively reducing SAR speckle, thereby improving the overall quality of glacier mapping results. Simultaneously, OBIA emerges as a robust framework for automated and accurate glacier mapping integrating diverse data sources such as InSAR and optical satellite imagery. Its contextual and hierarchical capabilities enable the implementation of customized rule sets tailored to specific mapping objectives, streamlining post-processing tasks and enhancing the ability to map various glacier surface types accurately. By combining InSAR coherence estimation and OBIA methods, we successfully delineated the Batura, Ghulkin, and Gulmit debris-covered glaciers, in the Hunza Valley. Our approach demonstrated reduced processing time and mapping errors while showcasing the potential for broader-scale glacier outline mapping. The almost global coverage and free availability of Sentinel-1 and Sentinel-2 data, along with their high temporal acquisition, make them ideal for studies with short temporal baselines and allow regular updates of global glacier databases promptly. For future studies, topographic data could also be integrated with InSAR coherence data and optical imagery in an OBIA approach to investigate its added value. This method allows for effectively mapping glacierized areas with extensive debris cover on a broader scale.

REFERENCES

Addink E.A., De Jong S.M., Pebesma E.J., 2007. *The importance of scale in object-based mapping of vegetation parameters with hyperspectral imagery.* Photogrammetric Engineering and Remote Sensing, 73 (8), 905-912. https://doi.org/10.14358/PERS.73.8.905

Alifu H., Tateishi R., Johnson B., 2015. *A new band ratio technique for mapping debris-covered glaciers using landsat imagery and a digital elevation model.* International Journal of Remote Sensing, 36 (8), 2063-2075. https://doi.org/10.1080/2150704X.2015.1034886

Anwar Y., Iqbal J., 2018. *Spatio temporal change of selected glaciers along Karakoram Highway from 1994-2017 using remote sensing and GIS techniques.* ISPRS Annals of the Photogrammetry, Remote Sensing and Spatial Information Sciences, 7-11. https://doi.org/10.5194/isprs-annals-IV-3-7-2018

Arigony-Neto J., Rau F., Saurer H., Jaña R., Simões J.C., Vogt S., 2007. *A time series of SAR data for monitoring changes in boundaries of glacier zones on the Antarctic Peninsula.* Annals of Glaciology, 46, 55-60. https://doi.org/10.3189/172756407782871387

Aubry-Wake C., Lamontagne-Hallé P., Baraër M., McKenzie J.M., Pomeroy J.W., 2023. *Using ground-based thermal imagery to estimate debris thickness over glacial ice: Fieldwork considerations to improve the effectiveness.* Journal of Glaciology, 69 (274), 353-569. https://doi.org/10.1017/jog.2022.67

Blaschke T., 2010. *Object based image analysis for remote sensing*. ISPRS Journal of Photogrammetry and Remote Sensing, 65 (1), 2-16. https://doi.org/10.1016/J.ISPRSJPRS.2009.06.004

Braun A., Veci L., 2021. *Sentinel-1 Toolbox Stripmap Interferometry Tutorial*. ESA, 27 pp. https://step.esa.int/docs/tutorials/S1TBX%20Stripmap%20Interferometry%20with%20Sentinel-1%20Tutorial_v2.pdf (last accessed: 08 October 2024)

Byers A.C., Rounce D.R., Shugar D.H., Lala J.M., Byers E.A., Regmi D., 2019. *A rockfall-induced glacial lake outburst flood, Upper Barun Valley, Nepal*. Landslides, 16 (3), 533-549. https://doi.org/10.1007/s10346-018-1079-9

Diolaiuti G., Fugazza D., Gallo M., Melis M., 2024. *The New Inventory of 13,032 Glacier in Pakistan: The "Glacier & Students" Project*. EvK2-CNR, Islamabad (Pakistan). 393 pp.

Frey H., Paul F., Strozzi T., 2012. *Compilation of a glacier inventory for the Western Himalayas from satellite data: Methods, challenges, and results*. Remote Sensing of Environment, 124, 832-843. https://doi.org/10.1016/j.rse.2012.06.020

Gamanya R., De Maeyer P., De Dapper M., 2009. *Object-oriented change detection for the city of Harare, Zimbabwe*. Expert Systems with Applications, 36 (1), 571-588. https://doi.org/10.1016/j.eswa.2007.09.067

Graham Cogley J., 2017. *Climate science: The future of Asia's glaciers*. Nature, 549 (7671), 166-167. https://doi.org/10.1038/549166a

Holobâcâ I.H., Tielidze L.G., Ivan K., Elizbarashvili M., Alexe M., Germain D., Petrescu S.H., Pop O.T., Gaprindashvili G., 2021. *Multi-sensor remote sensing to map glacier debris cover in the Greater Caucasus, Georgia*. Journal of Glaciology, 67 (264), 685-696. https://doi.org/10.1017/jog.2021.47

Jabbar A., Othman A.A., Merkel B., Hasan S.E., 2020. *Change detection of glaciers and snow cover and temperature using remote sensing and GIS: A case study of the Upper Indus Basin, Pakistan*. Remote Sensing Applications: Society and Environment, 18 (January), 100308. https://doi.org/10.1016/j.rsase.2020.100308

Jiang Z., Liu S., Wang X., Lin J., Long S., 2011. *Applying SAR interferometric coherence to outline debris-covered glacier*. Proceedings - 2011 19th International Conference on Geoinformatics, Geoinformatics 2011, 1-4. https://doi.org/10.1109/GeoInformatics.2011.5981184

Kääb A., Winsvold S.H., Altena B., Nuth C., Nagler T., Wuite J., 2016. *Glacier remote sensing using Sentinel-2. Part I: Radiometric and geometric performance, and application to ice velocity*. Remote Sensing, 8 (7). https://doi.org/10.3390/rs8070598

Kraaijenbrink P.D.A., Bierkens M.F.P., Lutz A.F., Immerzeel W.W., 2017. *Impact of a global temperature rise of 1.5 degrees Celsius on Asia's glaciers*. Nature, 549 (7671), 257-260. https://doi.org/10.1038/nature23878

Kraaijenbrink P.D.A., Shea J.M., Pellicciotti F., Jong S.M.D., Immerzeel W.W., 2016. *Object-based analysis of unmanned aerial vehicle imagery to map and characterise surface features on a debris-covered glacier*. Remote Sensing of Environment, 186, 581-595. https://doi.org/10.1016/j.rse.2016.09.013.

Lippl S., Vijay S., Braun M., 2018. *Automatic delineation of debris-covered glaciers using InSAR coherence derived from X-, C- and L-Band radar data: A case study of Yazgyl Glacier*. Journal of Glaciology, 64 (247), 811-821. https://doi.org/10.1017/jog.2018.70

Lu Z., Freymueller J.T., 1998. *Synthetic aperture radar interferometry coherence analysis over Katmai Volcano Group, Alaska*. Journal of Geophysical Research: Solid Earth, 103 (B12), 29887-29894. https://doi.org/10.1029/98jb02410

Massom R., Lubin D., 2006. *Polar Remote Sensing. Volume II: Ice Sheets*. Springer (Praxis Books / Geophysical Sciences), Berlin, 458 pp.

Mazhar N., Mirza A.I., Zia S., Butt Z.S., Shahid M.G., Mirza A.I., 2018. *An analysis of glacial retreat and resultant vegetation expansion in the Karakorum: A case study of Passu Glacier in Hunza Valley*. BBiologia (Lahore), 64 (1), 135-145. https://researcherslinks.com/current-issues/An-Analysis-of-Glacial-Retreat-and-Resultant-Vegetation/37/1/7285

Meyer F.J. (UAF/ASF)., 2020. *Sentinel-1 InSAR processing using the sentinel-1 Toolbox*, 21. https://asf.alaska.edu/wp-content/uploads/2019/05/generate_insar_with_s1tbx_v5.4.pdf (last access: 08 October 2024).

Michel J., Youssefi D., Grizonnet M., 2015. *Stable mean-shift algorithm and its application to the segmentation of arbitrarily large remote sensing images*. IEEE Transactions on Geoscience and Remote Sensing, 53 (2), 952-564. https://doi.org/10.1109/TGRS.2014.2330857

Moazzam M.F.U., Bae J., Lee B.G., 2022. *Impact of climate change on spatio-temporal distribution of glaciers in Western Karakoram Region since 1990: A case study of Central Karakoram National Park*. Water (Switzerland), 14 (19). https://doi.org/10.3390/w14192968

Mohajerani Y., Jeong S., Scheuchl B., Velicogna I., Rignot E., Milillo P., 2021. *Automatic delineation of glacier grounding lines in differential interferometric synthetic-aperture radar data using deep learning*. Scientific Reports, 11 (1), 1-10. https://doi.org/10.1038/s41598-021-84309-3

Nigrelli G., Chiarle M., Nuzzi A., Perotti L., Torta G., Giardino M., 2013. *A web-based, relational database for studying glaciers in the Italian Alps*. Computers and Geosciences, 51, 101-107. https://doi.org/10.1016/j.cageo.2012.07.027

Nuimura T., Sakai A., Taniguchi K., Nagai H., Lamsal D., Tsutaki S., Kozawa A., *et al.*, 2015. *The GAMDAM glacier inventory: A quality-controlled inventory of Asian glaciers*. Cryosphere, 9 (3), 849-864. https://doi.org/10.5194/tc-9-849-2015

Paul F., Winsvold S.H., Kääb A., Nagler T., Schwaizer G., 2016. *Glacier remote sensing using Sentinel-2. Part II: mapping glacier extents and surface facies, and comparison to Landsat 8*. Remote Sensing, 8 (7). https://doi.org/10.3390/rs8070575

Ranzi R., Grossi G., Iacovelli L., Taschner S., 2004. *Use of multispectral ASTER images for mapping debris-covered glaciers within the GLIMS Project*. International Geoscience and Remote Sensing Symposium (IGARSS), 2, 1144-1147. https://doi.org/10.1109/igarss.2004.1368616

Rastner P., Bolch T., Notarnicola C., Paul F., 2014. *A comparison of pixel- and object-based glacier classification with optical satellite images*. IEEE Journal of Selected Topics in Applied Earth Observations and Remote Sensing, 7 (3), 853-862. https://doi.org/10.1109/JSTARS.2013.2274668

Robson B.A., Nuth C., Dahl S.O., Hölbling D., Strozzi T., Nielsen P.R., 2015. *Automated classification of debris-covered glaciers combining optical, SAR and topographic data in an object-based environment*. Remote Sensing of Environment, 170, 372-387. https://doi.org/10.1016/j.rse.2015.10.001

Salvatore M.C., Zanoner T., Baroni C., Carton A., Banchieri F.A., Viani C., Giardino M., Perotti L., 2015. *The state of Italian glaciers: A snapshot of the 2006-2007 hydrological period*. Geografia Fisica e Dinamica Quaternaria, 38 (2), 175-198. https://doi.org/10.4461/GFDQ.2015.38.16

Shafique M., Faiz B., Bacha A.S., Ullah S., 2018. *Evaluating glacier dynamics using temporal remote sensing images: A case study of Hunza Valley, Northern Pakistan*. Environmental Earth Sciences, 77 (5), 1-11. https://doi.org/10.1007/s12665-018-7365-y

Shukla A., Arora M.K., Gupta R.P., 2010. *Synergistic Approach for mapping debris-covered glaciers using optical-thermal remote sensing data with inputs from geomorphometric parameters.* Remote Sensing of Environment, 114 (7), 1378-1387. https://doi.org/10.1016/j.rse.2010.01.015

Smith T., Bookhagen B., Cannon F., 2015. *Improving semi-automated glacier mapping with a multi-method approach: Applications in Central Asia.* Cryosphere, 9 (5), 1747-1759. https://doi.org/10.5194/tc-9-1747-2015

Stow D., Hamada Y., Coulter L., Anguelova Z., 2008. *Monitoring shrubland habitat changes through object-based change identification with airborne multispectral imagery.* Remote Sensing of Environment, 112 (3), 1051-1061. https://doi.org/10.1016/j.rse.2007.07.011

Thomas D.J., Robson B.A., Racoviteanu A., 2023. *An integrated deep learning and object-based image analysis approach for mapping debris-covered glaciers.* Frontiers in Remote Sensing, 4, 1-22. https://doi.org/10.3389/frsen.2023.1161530

Trias-Sanz R., Stamon G., Louchet J., 2008. *Using colour, texture, and hierarchial segmentation for high-resolution remote sensing.* ISPRS Journal of Photogrammetry and Remote Sensing, 63 (2), 156-168. https://doi.org/10.1016/j.isprsjprs.2007.08.005

Villarroya-Carpio A., Lopez-Sanchez J.M., Engdahl M.E., 2022. *Sentinel-1 interferometric coherence as a vegetation index for agriculture.* Remote Sensing of Environment, 280, 113208. https://doi.org/10.1016/j.rse.2022.113208

Wu H., Zhang Y., Zhang J., Lu Z., Zhong W., 2012. *Monitoring of glacial change in the head of the Yangtze River from 1997 to 2007 using Insar technique.* The International Archives of the Photogrammetry, Remote Sensing and Spatial Information Sciences, XXXIX-B7, 411-415. https://doi.org/10.5194/isprsarchives-xxxix-b7-411-2012

Xie F., Liu S., Gao Y., Zhu Y., Bolch T., Kääb A., Duan S., *et al.*, 2023. *Interdecadal glacier inventories in the Karakoram since the 1990s.* Earth System Science Data, 15 (2), 847-867. https://doi.org/10.5194/essd-15-847-2023